Michigan State University

National Superconducting Cyclotron Laboratory

REACTION DYNAMICS AND DEUTERON PRODUCTION

M.B. TSANG, P. DANIELEWICZ, D.R. BOWMAN,
N. CARLIN, C.K. GELBKE, Y.D. KIM, W.G. LYNCH,
L. PHAIR, R.T. de SOUZA, and F. ZHU

NSCL MSU

MSUCL-825

FEBRUARY 1992

MSUCL-825
February, 1992

Reaction Dynamics and Deuteron Production

M.B. Tsang, P. Danielewicz, D.R. Bowman, N. Carlin,[†]
C.K. Gelbke, Y.D. Kim,[*] W.G. Lynch, L. Phair,
R.T. de Souza,[*] and F. Zhu

National Superconducting Cyclotron Laboratory and
Department of Physics and Astronomy
Michigan State University, East Lansing, MI. 48824, USA

Abstract

Proton and deuteron azimuthal distributions with respect to the reaction plane have been measured as a function of associated charged-particle multiplicity for ^{36}Ar+^{197}Au collisions at E/A=35 MeV. Quantitative corrections for the dispersion of experimentally determined reaction planes about the true reaction plane have been applied. The results are compared to the predictions of a microscopic transport model which incorporates deuteron production and Coulomb effects.

PACS index: 25.70.Np

During the early stages of a nuclear collision, the initially highly ordered motion of projectile and target nucleons is dissipated and energy is fed into internal degrees of freedom. The process depends on the impact parameter of the collision and on the transition rates within the reacting system. Evidence for the persistence of collective motion throughout this nonequilibrium phase of the reaction [1-7] can be found in the enhanced emission of energetic particles in the entrance channel reaction plane [1,2,5-7]. Calculations [8,9] based on the Boltzmann-Uehling-Uhlenbeck (BUU) transport equation exhibit the expected dependence on impact parameter and, in addition, considerable sensitivity to the in-medium nucleon-nucleon cross section. Hence, significant constraints on reaction models may be supplied by measuring azimuthal distributions of emitted particles provided that the distributions are gated by an impact parameter filter.

Quantitative comparisons of measured and calculated azimuthal distributions must account for the resolution with which the reaction plane is determined experimentally. Standard techniques of filtering theoretical predictions by the response of the experimental apparatus are only valid for theories capable of predicting the triple differential cross sections of *all* particles employed in the reaction plane reconstruction. Since complex particles exhibit larger azimuthal anisotropies than nucleons [1,2,5-7], most experimental reaction plane reconstructions incorporate them into the analysis. This, however, makes it unfeasible to apply filtering techniques to macroscopic transport models like the BUU theory in which cluster emission is not treated reliably.

One can, however, extract the resolution of the experimental reaction plane determination from the data and unfold the measured azimuthal distributions to obtain distributions with respect to the "true" reaction plane [7].

In this letter, we apply this new approach to extract variances of proton and deuteron azimuthal distributions with respect to the true reaction plane as a function of the associated charged particle multiplicity. By relating the charged particle multiplicity to the impact parameter of the collision, we confront, for the first time, impact parameter (or multiplicity) selected experimental azimuthal distributions for protons *and* deuterons with microscopic calculations based upon the BUU theory [10,11].

The experiment was performed with a 35 MeV/nucleon ^{36}Ar beam from the K1200 cyclotron of Michigan State University bombarding a ^{197}Au target of 1 mg/cm^2 areal density. Charged particles were detected with the MSU Miniball [12], a plastic-CsI(Tl) scintillator phoswich detector array which covered angles of $16° \leq \theta_{lab} \leq 160°$, corresponding to 85% of 4π. Isotopic identification was achieved for p, d, t, ^{3}He, and ^{4}He. Heavier particles were identified by atomic number up to Z≈20. Representative energy thresholds for identified particles are $E_{th}/A \approx 2$, 3, and 4 MeV for He, Ne, and Ar, respectively. Further experimental details are given in refs. [7,12,13].

Impact parameter averaged differential multiplicity distributions for protons and deuterons detected at $\theta=45°$ and 130° are shown in Fig. 1. The emission patterns are strongly forward peaked, indicating the dominance of pre-equilibrium processes at forward angles. However, collective effects are difficult to unravel from the inclusive spectra [2]. They are readily discerned in the azimuthal emission patterns.

To extract the azimuthal distributions of a given "trigger" particle with respect to the "true" reaction plane, we have followed the procedure outlined in ref. 7. For each event with N-1 identified charged particles detected in coincidence with the trigger particle, we define [5-7] the "reconstructed" reaction plane as the plane spanned by the beam axis and the major axis of the transverse momentum tensor for the N-1 coincident particles [14]. The azimuthal angle, Φ, of the reconstructed reaction plane then minimizes the sum [5-7],

$$\Sigma_p(\Phi) = \sum_{i=1}^{N-1} p_i^2 \sin^2\theta_i \sin^2(\phi_i - \Phi) . \tag{1}$$

In Eq. 1, p_i, θ_i, and ϕ_i denote the momentum, polar and azimuthal angles of particle i in the laboratory system. (The beam axis defines θ=0°.)

As an example, the solid points in Fig. 2 show "raw" azimuthal distributions, $P_r(\phi=|\phi_N-\Phi|)$, relative to the reconstructed reaction plane [7,15]. The left and right hand panels show distributions measured for protons and deuterons, respectively, emitted at θ=45° and selected by the multiplicity cut of N=9. In order to provide a meaningful test of microscopic transport models, one must minimize contributions of evaporative emission from equilibrated target-like residues. Therefore, energy thresholds of E(p)≥32 MeV and E(d)≥40 MeV were imposed on the trigger particle. Consistent with previous findings, emission is strongly enhanced in the reconstructed reaction plane; such collective effects are more pronounced for deuterons than for protons [1-7].

Due to fluctuations of the angle between reconstructed and true reaction planes, the experimental azimuthal anisotropies, as shown in Fig. 2, are smaller than anisotropies with respect to the true reaction plane. Following refs. [7,17], we have estimated the dispersion of reconstructed reaction planes about the true reaction plane by randomly subdividing each event into two subevents, each containing half of the N-1 associated charged particles. Figure 3 shows $\mathbf{P}(\Phi_{12})$, the distribution of angles Φ_{12} between the two planes extracted (in analogy to Eq. 1) for the two sub-events. Under the assumption of statistical independence of sub-events, the distribution $\mathbf{P}(\Phi_{12})$ is related to the distribution $\mathbf{P}_{½}(\Phi)$ of relative orientations Φ between the true reaction plane and the planes reconstructed from the sub-events [7]:

$$\mathbf{P}(\Phi_{12}) = \int \mathbf{P}_{½}(\Phi)\mathbf{P}_{½}(\Phi+\Phi_{12})d\Phi \,. \tag{2}$$

The solid line in Fig. 3 shows the convolution obtained with the ansatz [7]

$$\mathbf{P}_{½}(\Phi) = \exp(-\omega^2 \sin^2\Phi) \,. \tag{3}$$

The function $\mathbf{P}_{½}(\Phi)$ is depicted by the dot-dashed curve in the figure. The accuracy of reaction plane reconstruction is improved by using the full set of N-1 particles instead of the subset of ½(N-1) particles. Monte-Carlo calculations indicate that this increase in accuracy may be readily assessed without sensitivity to detailed assumptions about the distribution of emitted particles [7,17]. This improvement in accuracy is illustrated by the dashed curve in Fig. 3 which depicts $\mathbf{P}(\Phi)$, the distribution of reaction planes reconstructed from the full set of N-1 associated particles.

For the emitted light particles, the raw azimuthal distributions $P_r(\phi)$ and the "true" distributions $P_t(\phi)$ with respect to the true reaction plane are related by the convolution [7]

$$P_r(\phi) = \int P_t(\Phi+\phi)\mathbf{P}(\Phi)d\Phi \,. \tag{4}$$

Good accuracy is achieved [7] by approximating $P_t(\phi)$ and $\mathbf{P}(\Phi)$ by the functional form given on the right hand side of Eq. 3. The resulting fits and extracted distribution $P_t(\phi)$ are given by the solid and dot-dashed curves in Fig. 2, respectively.

To allow a compact presentation of the multiplicity dependence of the azimuthal distributions, we have determined the variances of the true distributions $P_t(\phi)$:

$$<\phi^2>^{1/2} = [\int \phi^2 P_t(\phi)d\phi/(\int P_t(\phi)d\phi)]^{1/2}, \qquad (5)$$

where the integration is over the interval $0 \le \phi \le \pi/2$. The results are shown in Fig. 4. Following ref. [13], we have assumed a monotonic relationship between charged particle multiplicity and impact parameter; the corresponding impact parameters are given as the upper scale of Fig. 4. For both protons and deuterons, the extracted variances increase with charged particle multiplicity indicating increasingly isotropic distributions for decreasing impact parameters. Qualitatively this trend is expected. For impact parameter b=0, the emission must be azimuthally isotropic. However, the extracted variances of the deuteron distributions at large N are smaller than $<\phi^2>^{1/2} \approx 52°$, the variance of an isotropic distribution. This discrepancy may reflect some imprecision in the impact parameter selection.

To explore whether the extracted azimuthal variances can be reproduced by microscopic transport models, we performed calculations within the framework of a modified BUU model [11] capable of predicting proton *and* deuteron production. This model provides reasonable descriptions of d/p ratios and of spectra at bombarding energies of 100 $\text{MeV} \lesssim E/A \lesssim 2$ GeV [11]. As in other work [8-10], we adopted a parametrization of the optical potential in terms of a local density, representing a soft equation of state (EOS) with compressibility K=200 MeV. Coulomb interactions were taken into account. The elastic in-medium nucleon-nucleon cross section was taken as the experimental free nucleon-nucleon scattering cross section. The calculations were terminated at the collision time of 220 fm/c. Remaining Coulomb effects were incorporated by adding the potential energy in the Coulomb field of a residual system to the kinetic energy of emitted particles.

Inclusive spectra predicted by the model are shown in Fig. 1. The predicted multiplicities were adjusted to the data by multiplication with a factor of 0.5. This renormalization is reasonable since the present calculations do not include the loss of flux due to emission of heavier clusters (t, ^{3}He, α, ...). The calculated relative cross sections agree reasonably with the data. At θ=45°, the calculations predict somewhat steeper spectra than observed experimentally; at θ=130°, the trend is reversed.

The variances of azimuthal distributions are not subject to normalization uncertainties. In Fig. 4, the predicted azimuthal variances of protons and deuterons are shown as solid diamonds. The calculations were performed for the impact parameters given by the top scale. The predicted impact parameter dependence is less pronounced than observed experimentally. Overall, the agreement between theory and experiment is satisfactory. However, for larger impact parameters the predicted azimuthal variances of deuterons are larger than observed. Different choices of the equation of state and/or the in-medium cross sections may improve the agreement between data and theory.

In order to assess the importance of Coulomb distortions on the predicted azimuthal variances, we have also performed calculations in which Coulomb interactions are neglected (open diamonds). Consistent with previous calculations in which Coulomb effects were neglected [8,9], the predicted azimuthal variances exhibit a characteristic "V"-shape as a function of impact parameter. This "V"-shape bears little resemblance to the measured multiplicity dependence of the azimuthal variances. While this discrepancy makes quantitative comparisons difficult, these calculations nevertheless reproduce the rough order of magnitude of the measured azimuthal variances.

In summary, proton and deuteron azimuthal distributions for ^{36}Ar induced reactions on ^{197}Au have been measured relative to the entrance channel reaction plane. These distributions are strongly enhanced in the reaction plane for peripheral collisions, but become more isotropic for central collisions. BUU calculations indicate that Coulomb interactions cannot be neglected in quantitative comparisons with experimental data. While the present calculations reproduce the overall magnitude of the observed azimuthal anisotropies, some quantitative discrepancies remain.

This paper is based upon work supported by the National Science Foundation under Grant numbers PHY-84-51280, PHY-89-13815, PHY-89-05933, and PHY-90-17077. WGL acknowledges the receipt of a U.S. Presidential Young Investigator Award.

References

† Present address: Instituto de Física, Universidade de São Paulo, C. Postal 20516, CEP 01498, São Paulo, Brazil

* Present address: Indiana University Cyclotron Facility and Department of Chemistry, Indiana University, Bloomington, IN 47405

1. M.B. Tsang, C.B. Chitwood, D.J. Fields, C.K. Gelbke, D.R. Klesch, W.G. Lynch, K. Kwiatkowski and V.E. Viola, Jr., Phys. Rev. Lett. 52, 1967 (1984).
2. C.B. Chitwood, D.J. Fields, C.K. Gelbke, D.R. Klesch, W.G. Lynch, M.B. Tsang, T.C. Awes, R.L. Ferguson, F.E. Obenshain, F. Plasil, R.L. Robinson, and G.R. Young, Phys. Rev. C34, 858 (1986).
3. M.B. Tsang, R.M. Ronningen, G. Bertsch, Z. Chen, C.B. Chitwood, D.J. Fields, C.K. Gelbke, W.G. Lynch, T. Nayak, J. Pochodzalla, T. Shea, and W. Trautmann, Phys. Rev. Lett. 57, 559 (1986).
4. M.B. Tsang, W.G. Lynch, R.M. Ronningen, Z. Chen, C.K. Gelbke, T. Nayak, J. Pochodzalla, F. Zhu, M. Tohyama, W. Trautmann, and W. Dünnweber, Phys. Rev. Lett. 60, 1479 (1988).
5. W.K. Wilson, W. Benenson, D.A. Cebra, J. Clayton, S. Howden, J. Karn, T. Li, C.A. Ogilvie, A. Vander Molen, G.D. Westfall, J.S. Winfield, and A. Nadasen, Phys. Rev. C41, R1881 (1990).
6. W.K. Wilson, R. Lacey, C.A. Ogilvie, and G.D. Westfall, Phys. Rev. C45, 738 (1992).
7. M.B. Tsang, R.T. de Souza, Y.D. Kim, D.R. Bowman, N. Carlin, C.K. Gelbke, W.G. Gong, W.G. Lynch, L. Phair, and F. Zhu, Phys. Rev. C44, 2065 (1991).
8. M.B. Tsang, G.F. Bertsch, W.G. Lynch, and M. Tohyama, Phys. Rev. C40, 1685 (1989).

9. H.M. Xu, W.G. Lynch, P. Danielewicz, and G.F. Bertsch, Phys. Rev. Lett. 65, 843 (1990).

10. G.F. Bertsch and S. Das Gupta, Phys. Rep. 160, 189 (1988), and refs. given there.

11. P. Danielewicz and G.F. Bertsch, Nucl. Phys. A533, 712 (1991).

12. R.T. de Souza, N. Carlin, Y.D. Kim, J. Ottarson, L. Phair, D.R. Bowman, C.K. Gelbke, W.G. Gong, W.G. Lynch, R.A. Pelak, T. Peterson, G. Poggi, M.B. Tsang, and H.M. Xu, Nucl. Instr. and Meth. A295, 109 (1990).

13. Y.D. Kim, R.T. de Souza, D.R. Bowman, N. Carlin, C.K. Gelbke, W.G. Gong, W.G. Lynch, L. Phair, M.B. Tsang, and F. Zhu, Phys. Rev. C45, 338 (1992).

14. Excluding the "trigger" particle avoids self-correlations. Corrections for momentum conservation effects were applied as discussed in ref. [7].

15. For convenience, the distributions are normalized at P(0)=1.

16. P. Danielewicz and G. Odyniec, Phys. Lett. B157, 146 (1985).

17. In the limit of very large values of N, the variance would decrease by $1/\sqrt{2}$, in accordance with the central limit theorem.

Figure Captions

Fig. 1: Energy spectra for protons (left) and deuterons (right) detected at θ_{lab}=45° (solid points) and θ_{lab}=130° (open points). The solid curves represent results from BUU calculations.

Fig. 2: The points show azimuthal distributions, $P_r(\phi)$, of protons (left) and deuterons (right) relative to the reconstructed reaction plane. The dot-dashed curves represent extracted distributions, $P_t(\phi)$, relative to the true reaction plane. The solid curves depict the convolutions (Eq. 4) of $P_t(\phi)$ with $\mathbf{P}(\Phi)$, the distribution of angles between the reconstructed and true reaction planes.

Fig. 3: The points show the measured distributions for the relative azimuthal angle, Φ_{12}, between planes determined by two sub-events of multiplicity ½(N-1). The solid and dot-dashed curves represent the distributions $\mathbf{P}(\Phi_{12})$ and $\mathbf{P}_{½}(\Phi)$ related via Eq. 2. The dashed curve represents the distribution $\mathbf{P}(\Phi)$ for the angles between the reconstructed and true reaction planes .

Fig. 4: Variances of the azimuthal distributions relative to the true reaction plane. Solid circular points: extracted dependence on raw charged particle multiplicity. Solid and open diamonds: impact parameter dependence predicted by BUU calculations which do and do not include Coulomb interactions, respectively. The multiplicity and impact parameter scales in the figure are related according to the geometrical prescription of ref. [13].

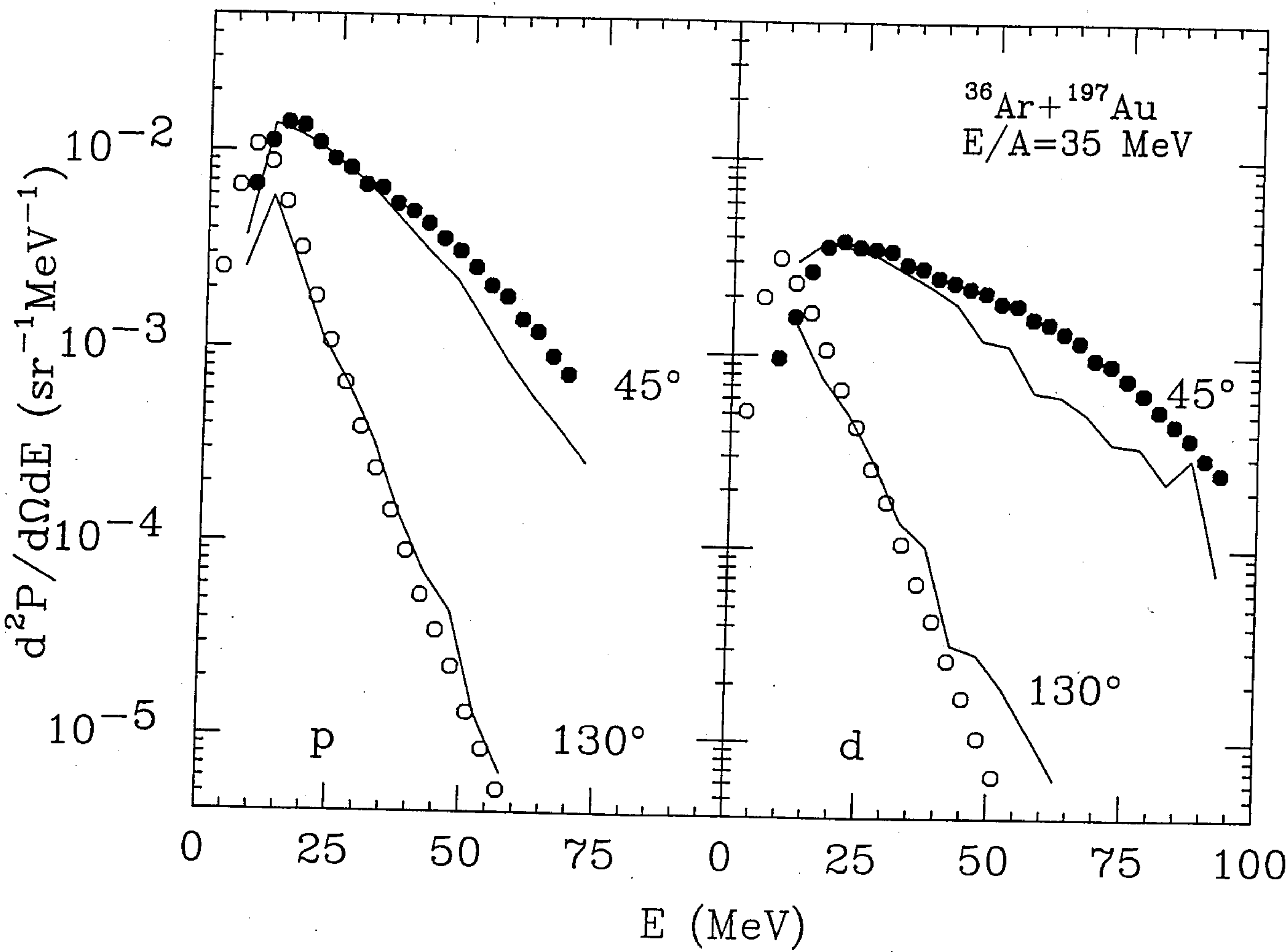
36Ar+197Au
E/A=35 MeV
d2P/dΩdE (sr−1MeV−1)
10−2
10−3
10−4
10−5
45°
130°
p
d
0
25
50
75
100
E (MeV)

Fig. 1

MSU-92-008

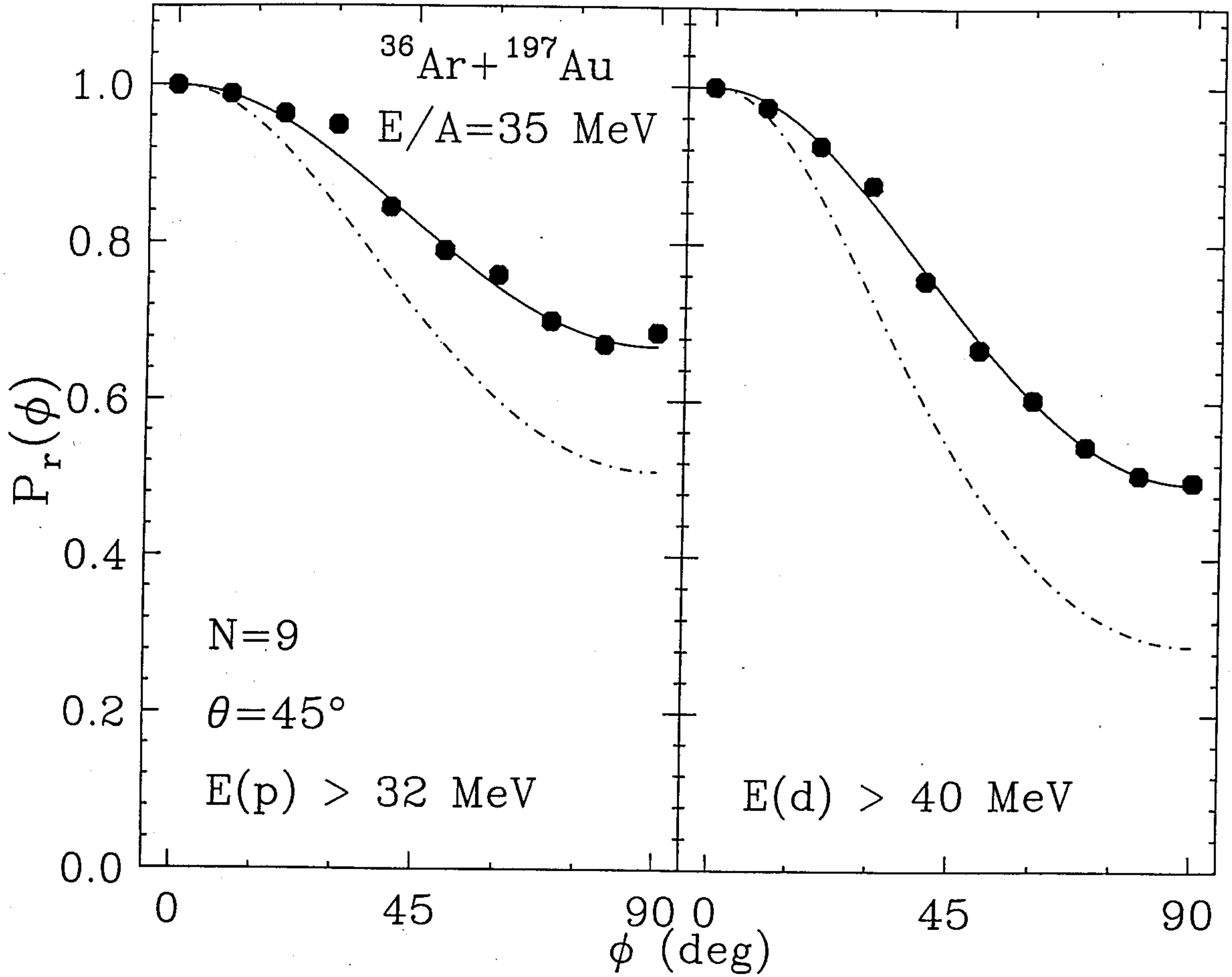

Fig. 2

MSU-92-009

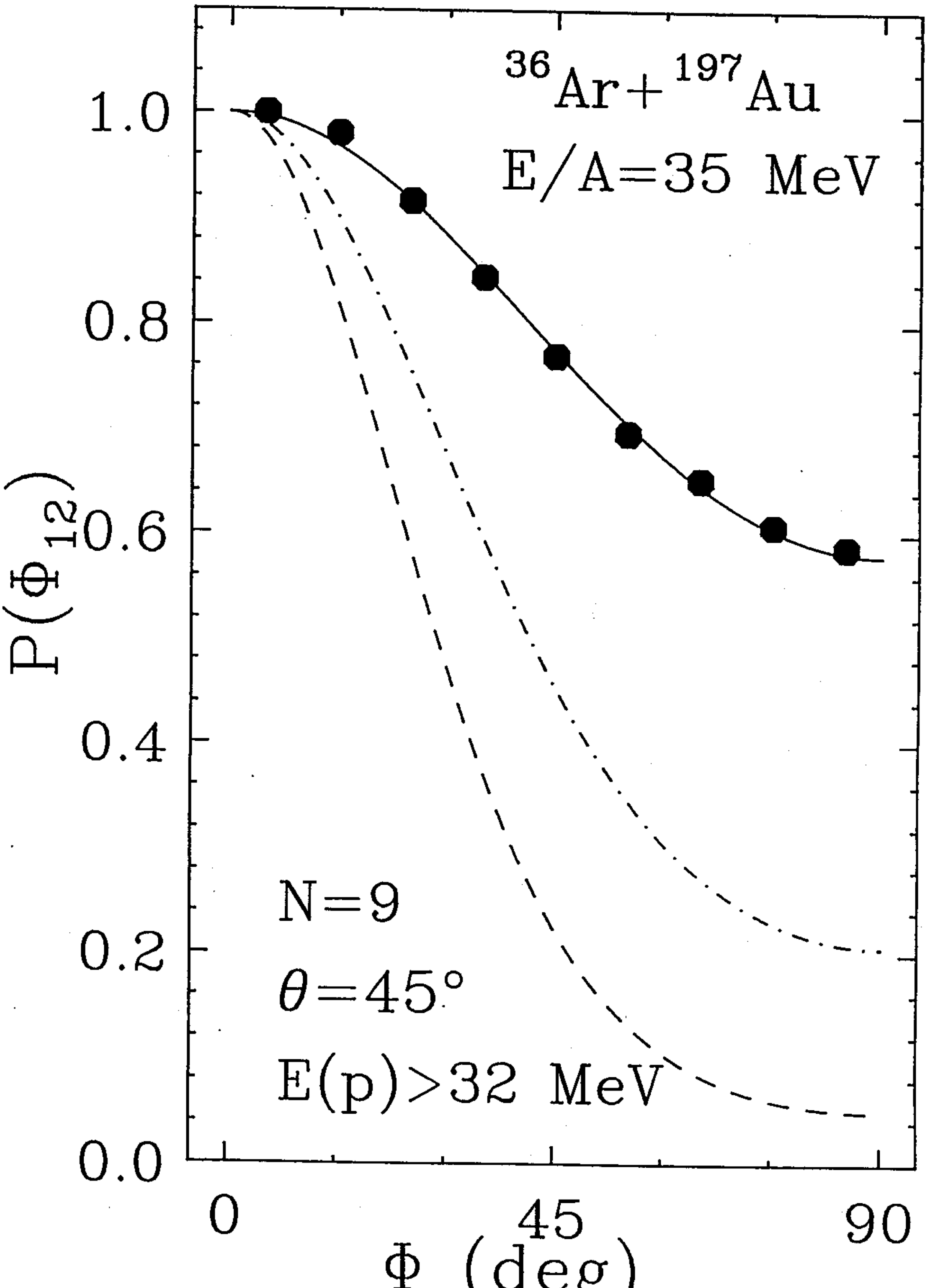

Fig. 3

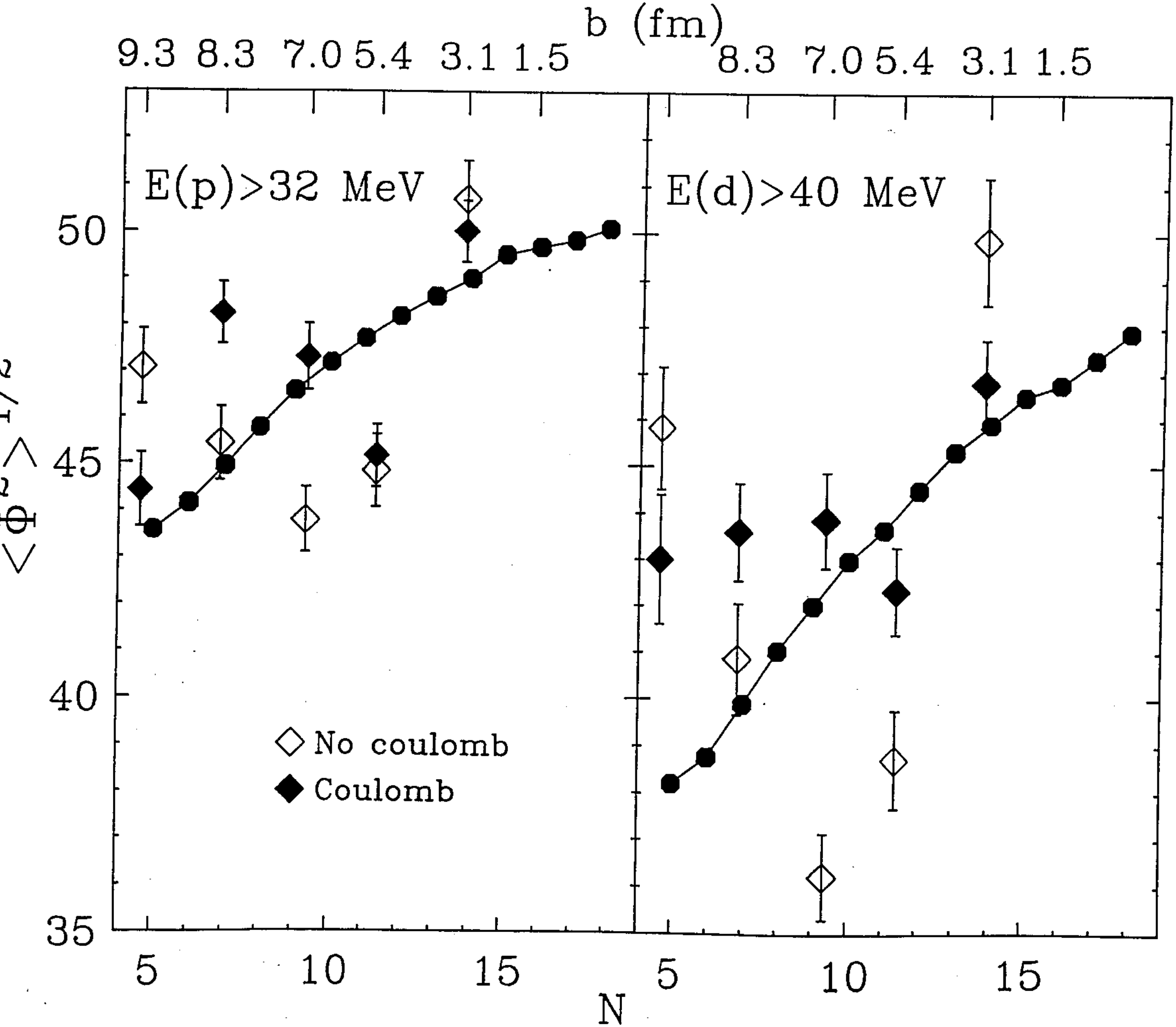
b (fm)
9.3 8.3 7.0 5.4 3.1 1.5
8.3 7.0 5.4 3.1 1.5
E(p)>32 MeV
E(d)>40 MeV
$\langle \Phi^2 \rangle^{1/2}$
50
45
40
35
No coulomb
Coulomb
5
10
15
N

Fig. 4